Oscillations of two-dimensional solitons in harmonic and Bessel optical lattices

Yaroslav V. Kartashov,[1,2] Victor A. Vysloukh,[3] and Lluis Torner[1]
[1]*ICFO–Institut de Ciencies Fotoniques, and Department of Signal Theory and Communications, Universitat Politecnica de Catalunya, 08034 Barcelona, Spain*
[2]*Department of Physics, M. V. Lomonosov Moscow State University, 119899, Moscow, Russia*
[3]*Departamento de Fisica y Matematicas, Universidad de las Americas—Puebla, Santa Catarina Martir, 72820, Puebla, Cholula, Mexico*
(Received 8 November 2004; published 28 March 2005)

We consider parametric amplification of two-dimensional spatial soliton oscillations in longitudinally modulated harmonic and Bessel lattices in Kerr-type saturable medium. We show that soliton center oscillations along different axes in two-dimensional lattices are coupled, which gives rise to a number of interesting propagation scenarios including periodic damping and excitation of soliton oscillations along perpendicular axes, selective amplification of soliton oscillations along one transverse axis, and enhancement of soliton spiraling.

DOI: 10.1103/PhysRevE.71.036621 PACS number(s): 42.65.Tg, 42.65.Wi, 42.65.Jx

Solitons in optically induced lattices were predicted and experimentally observed in photorefractive crystals in one and two transverse dimensions [1–4]. In photorefractive materials harmonic lattices are usually formed by the interference pattern of several plane waves whose intensity and intersection angles define the lattice depth and period. Such lattices may be used for engineering of systems with tunable discreteness since they can operate in both regimes of weak and strong coupling between neighboring sites depending on the depth and period of refractive index modulation. Analogously to their discrete counterparts [5], lattice solitons can be used for a number of practical applications including all-optical switching and power-dependent soliton steering [6]. Properties of single solitons and soliton complexes supported by one- and two-dimensional optical lattices are now well established [7–13]. Lately, we have addressed properties of solitons supported by radially symmetric Bessel lattices [14]. Such lattices could be photoinduced by nondiffracting zero-order Bessel beams and offer many new opportunities including control of soliton interactions in different lattice rings and the possibility to set solitons into controllable rotary motion.

It was demonstrated recently that the presence of shallow *longitudinal* modulation of linear refractive index profoundly affects properties of solitons trapped in the guiding channel of a one-dimensional optical lattice [15,16]. In particular, parametric amplification of transverse oscillations and amplitude oscillations of spatial solitons is possible under appropriate conditions. The former effect can be potentially used for controllable soliton steering and fine-tuning of soliton inclination angle at the output face of the crystal. Two-dimensional generalization of this technique is far from being trivial because of the presence of the second transverse dimension, hence more complicated soliton trajectories. Moreover, despite the fact that in the absence of longitudinal modulation harmonic and Bessel lattices can support stable two-dimensional solitons even in a cubic medium, the open question is whether a two-dimensional soliton is sufficiently robust to survive under remarkable longitudinal modulation of the linear refractive index which is necessary for effective parametric amplification of the soliton oscillations.

In this paper we show that a considerable parametric amplification of soliton oscillations can be achieved in the two-dimensional case when small nonlinearity saturation is taken into account. We have found that transverse oscillations of the soliton center are coupled even in the absence of longitudinal modulation. This coupling is strong if frequencies of soliton beam oscillations along both transverse axes coincide; otherwise, it is weak and parametric amplification of soliton center oscillations along a selected axis is possible. We discuss some potential practical applications of parametric amplification of soliton oscillations.

Our analysis is based on the nonlinear Schrödinger equation describing propagation of a laser beam in a medium with focusing Kerr-type saturable nonlinearity and spatial modulation of refractive index along longitudinal and transverse directions

$$i\frac{\partial q}{\partial \xi} = -\frac{1}{2}\left(\frac{\partial^2 q}{\partial \eta^2} + \frac{\partial^2 q}{\partial \zeta^2}\right) - \frac{q|q|^2}{1+S|q|^2} - pQ(\xi)R(\eta,\zeta)q. \quad (1)$$

Here, $q(\eta,\zeta,\xi)$ is the slowly varying dimensionless complex amplitude of the light field, transverse η,ζ, and longitudinal ξ coordinates are scaled in terms of beam radius and diffraction length, respectively, S is the saturation parameter, guiding parameter p is proportional to the refractive index modulation depth in the transverse direction, and the functions $R(\eta,\zeta)$ and $Q(\xi)$ describe transverse and longitudinal refractive index profiles. Further, we suppose that longitudinal variation of refractive index is described by the harmonic function $Q(\xi)=1-\mu\cos(\Omega_\xi \xi)$, where the parameter $\mu<1$ and Ω_ξ is the spatial frequency of longitudinal refractive index modulation. We consider two types of transverse profiles of refractive index: the harmonic one with $R_H(\eta,\zeta)=\cos(\Omega_\eta\eta)\cos(\Omega_\zeta\zeta)$, where Ω_η,Ω_ζ are transverse spatial modulation frequencies, and the Bessel one $R_B(\eta,\zeta)=J_0((2b_{lin})^{1/2}r)$, where $r=(\eta^2+\zeta^2)^{1/2}$ is the radius, and parameter b_{bin} is the corresponding scaling factor [see Fig. 1(a) and 1(b)]. The depth of refractive index modulation is as-

 ©2005 The American Physical Society

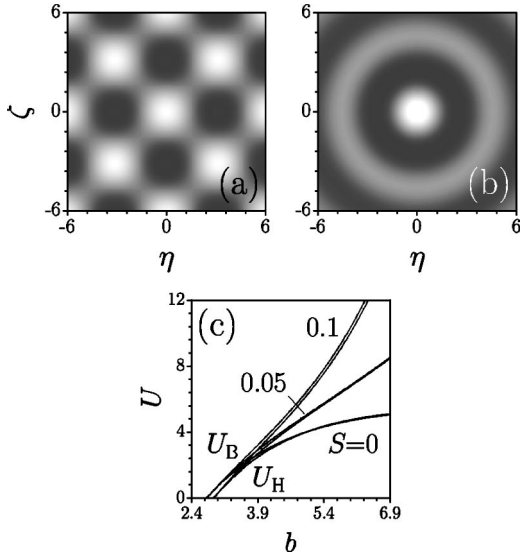

FIG. 1. (a) Harmonic and (b) Bessel optical lattices. Harmonic lattice is shown for $\Omega_\eta=\Omega_\zeta=1$, while Bessel lattice corresponds to $b_{\mathrm{lin}}=1.172$. (c) Energy flow versus propagation constant for solitons supported by Bessel (U_B) and harmonic (U_H) lattices at different values of saturation parameter and $p=5$. All quantities are plotted in arbitrary dimensionless units.

sumed to be small compared with the unperturbed refractive index, and is of the order of nonlinear contribution due to the Kerr effect. Longitudinal modulation is supposed to be weak and smooth, which enables one to neglect the reflected wave. In practice, the refractive index modulation in the transverse direction can be induced optically in photorefractive crystals with several interfering plane waves [1–4] or with nondiffracting Bessel beams [14]. Longitudinal modulation can be created in such media with spatially periodic background illumination along the ξ axis. Though in the case of real photorefractive crystal the model equation describing soliton propagation would be more complicated than Eq. (1), since the refractive index profile will also depend on the level of saturation, we expect that simplified model (1) adequately describes the main qualitative features of soliton oscillations. Notice that the total energy flow

$$U=\int_{-\infty}^{\infty}\int_{-\infty}^{\infty}|q|^2 d\eta d\zeta, \tag{2}$$

remains constant upon propagation.

In the absence of longitudinal refractive index modulation, Eq. (1) possesses soliton solutions [7–14]. Here, we recall basic properties of fundamental solitons. Soliton solutions can be found in the form $q(\eta,\zeta,\xi)=w(\eta,\zeta)\exp(ib\xi)$, where $w(\eta,\zeta)$ is the real function, and b is the propagation constant. Substitution of this expression into Eq. (1) yields

$$\frac{1}{2}\left(\frac{\partial^2 w}{\partial\eta^2}+\frac{\partial^2 w}{\partial\zeta^2}\right)+\frac{w^3}{1+Sw^2}+pR(\eta,\zeta)w-bw=0. \tag{3}$$

Mathematically, families of soliton solutions of Eq. (3) are defined by parameters p,S,b, and transverse configuration of the lattice. Thus, the fundamental soliton supported by the Bessel lattice is radially symmetric and the position of its intensity maximum coincides with the center of the lattice, while in harmonic lattices the soliton can be supported by either guiding site of the lattice. Here, we found corresponding soliton profiles numerically using the standard relaxation method. Typically we used a discretization scheme with 1024×1024 points per soliton profile; the transverse step was set to $d\eta=d\zeta=0.02$. Zero boundary conditions were implemented. The progressive iterations in the relaxation method were carried out until the relative difference between profiles on two successive iterations decreased below 10^{-20}. The accuracy of calculations was checked by doubling the number of points per profile as well as by expanding the computation window (for broad solitons). The energy flow of solitons supported by Bessel and harmonic lattices versus propagation constant is shown in Fig. 1(c) for different values of the saturation parameter. For convenience of comparison we selected the scaling factor b_{lin} for the Bessel lattice in such a way that the first zero of the Bessel lattice coincides with that of the harmonic one [Fig. 1(a) and 1(b)]. Energy flows $U_{B,H}$ of solitons supported by lattices of both types grow monotonically with increase of b, which indicates soliton stability [14] for chosen lattice parameters. Dispersion curves $U_B(b)$ and $U_H(b)$ are quite similar and differ notably only near a lower cutoff for soliton existence where the soliton spreads over many lattice sites and exact periodicity of harmonic lattice and decaying behavior of the tail of the Bessel lattice play a crucial role. As one can see from Fig. 1(c), the cutoff for solitons supported by Bessel lattices is a bit lower than that for solitons in harmonic lattices.

While exact solitons whose intensity maximum position coincides with the maximum of the lattice will propagate in a stable way without any distortions, the small transverse displacement or tilt of the input soliton with respect to the lattice causes oscillations of the beam center in the transverse plane upon propagation. Further, for illustration of the main propagation scenarios of solitons in modulated lattices we solve Eq. (1) with an input condition

$$q(\eta,\zeta,\xi=0)=w(\eta-\eta_0,\zeta-\zeta_0)\exp(i\alpha_\eta\eta+i\alpha_\zeta\zeta), \tag{4}$$

where $w(\eta,\zeta)$ is the exact soliton solution, η_0,ζ_0 are initial shifts along the η- and ζ axes, and α_η,α_ζ are input angles.

To understand multidimensional dynamics of tilted or shifted soliton beams in optical lattices, one can use an effective particle approach [15,16], based on equations of motion for integral coordinates of the beam center

$$\frac{d^2}{d\xi^2}\langle\eta\rangle=p\frac{Q(\xi)}{U}\int_{-\infty}^{\infty}\int_{-\infty}^{\infty}|q|^2\frac{\partial R}{\partial\eta}d\eta d\zeta,$$
$$\frac{d^2}{d\xi^2}\langle\zeta\rangle=p\frac{Q(\xi)}{U}\int_{-\infty}^{\infty}\int_{-\infty}^{\infty}|q|^2\frac{\partial R}{\partial\zeta}d\eta d\zeta. \tag{5}$$

Here, integral coordinates $\langle\eta\rangle=U^{-1}\int_{-\infty}^{\infty}\int_{-\infty}^{\infty}\eta|q|^2\,d\eta d\zeta$ and $\langle\zeta\rangle=U^{-1}\int_{-\infty}^{\infty}\int_{-\infty}^{\infty}\zeta|q|^2\,d\eta d\zeta$, and Eq. (5) are derived in the limit of cubic nonlinearity at $S\to0$. The approach requires the substitution of a trial expression for the beam profile in the right sides of Eq. (5). We use Gaussian beam

$|q(\eta,\zeta,\xi)| = q_0 \exp[-\chi_\eta^2(\eta - \langle\eta\rangle)^2]\exp[-\chi_\zeta^2(\zeta - \langle\zeta\rangle)^2]$, where χ_η, χ_ζ are form factors and q_0 is the amplitude. In the simplest case of harmonic lattice, one gets

$$\frac{d^2}{d\xi^2}\langle\eta\rangle + [1 - \mu\cos(\Omega_\xi\xi)]W_G\Omega_\eta\cos(\Omega_\zeta\langle\zeta\rangle)\sin(\Omega_\eta\langle\eta\rangle) = 0,$$
$$\frac{d^2}{d\xi^2}\langle\zeta\rangle + [1 - \mu\cos(\Omega_\xi\xi)]W_G\Omega_\zeta\cos(\Omega_\eta\langle\eta\rangle)\sin(\Omega_\zeta\langle\zeta\rangle) = 0. \quad (6)$$

Here, the parameter

$$W_G = p\exp[-(\Omega_\eta^2/\chi_\eta^2 + \Omega_\zeta^2/\chi_\zeta^2)/4], \quad (7)$$

depends on the ratio between the characteristic lattice and beam scales, as well as on the depth of the lattice. In optically induced lattices this parameter can be fine-tuned by changing the lattice depth. This enables one to control dynamics of soliton motion effectively inside the lattice for the same input profiles. Notice that other trial expressions for beam profile lead to very similar equations for soliton center coordinates. As one can see from Eq. (6), there is a straightforward analogy between equations of soliton movement in harmonic lattice and equations of motion for coupled parametrically driven pendulums. For the simplest case, $\mu=0$ and small initial soliton center displacements along η and ζ axes, oscillations in these directions are independent, almost periodic, and occur at certain frequencies given by $W_G^{1/2}\Omega_\eta$ and $W_G^{1/2}\Omega_\zeta$, respectively, that can be termed frequencies of free oscillations. Notice that for the Bessel lattice the frequency of free oscillations Ω_0 is unique because of the radial symmetry of the lattice. For the case of relatively narrow solitons ($b_{\rm lin}^{1/2} \ll \chi_\eta, \chi_\zeta$) this frequency can be roughly estimated as $\Omega_0 \approx (pb_{\rm lin})^{1/2}\exp[-b_{\rm lin}/4\chi_\eta^2]$, assuming that $\chi_\eta = \chi_\zeta$.

However, even at $\mu=0$ large-amplitude oscillations of the soliton center along the η- and ζ axes become coupled. This is an essentially new feature of two-dimensional soliton oscillations in optical lattices in comparison with this phenomenon in one-dimensional lattices [15]. If large-amplitude oscillations along the η axis occur approximately at the same frequency as small-amplitude ones along the ζ axis (i.e., when $\Omega_\eta = \Omega_\zeta$), the parametric resonance arises. Such parametric-type interaction opens an opportunity to transform effectively large-amplitude η oscillations into oscillations along the ζ axis [Fig. 2(a)]. This process repeats periodically in ξ and looks like amplitude beatings. Notice that under appropriate conditions predictions of the effective particle model [Eq. (6)] are in a reasonable agreement with results of direct integration of Eq. (1) with input conditions (4). Thus, at $\mu=0$, $\Omega_\eta=\Omega_\zeta=1$, $p=6$, $\eta_0=1$, $\zeta_0=0.1$, $\alpha_\eta=\alpha_\zeta=0$, and for a soliton beam corresponding to $b=7$ and $S=0.1$, the difference between oscillation beating length $L_b \approx 47.9$ obtained from Eq. (1) and L_b obtained on the basis of Eq. (6) for the Gaussian input beam with the same energy flow is about 13%.

A more complicated situation occurs in lattices with longitudinal refractive index modulation. In such lattices the soliton center starts to oscillate with exponentially growing amplitude provided that the first parametric resonance condition $\Omega_\xi \approx 2\Omega_0$ is satisfied (here, Ω_0 is the frequency of free oscillations). The simplest case corresponds to the absence of coupling between η- and ζ oscillations. This can be achieved when the soliton is initially shifted along only one of the transverse axes and oscillations occur in one plane [Fig. 2(b)]. Notice that growth of the oscillation amplitude leads to diminishing of the instantaneous frequency, and the system escapes from the condition of parametric resonance. This results in periodic in ξ decay and growth of soliton oscillations (or beatings). In this case the effective particle approach also offers quite a realistic estimate for beating length and maximal value of transverse displacement of the soliton center. For example, at $\mu=0.1$, $\Omega_\eta=\Omega_\zeta=1$, $p=6$, $\eta_0=0.1$, $\zeta_0=0$, $\alpha_\eta=\alpha_\zeta=0$, and for a soliton with $b=7$, $S=0.1$, the relative difference in calculation of beating length in the frames of two approaches is around 11%, and accuracy of calculation of the maximal value of transverse displacement of the soliton center is around 2.5%.

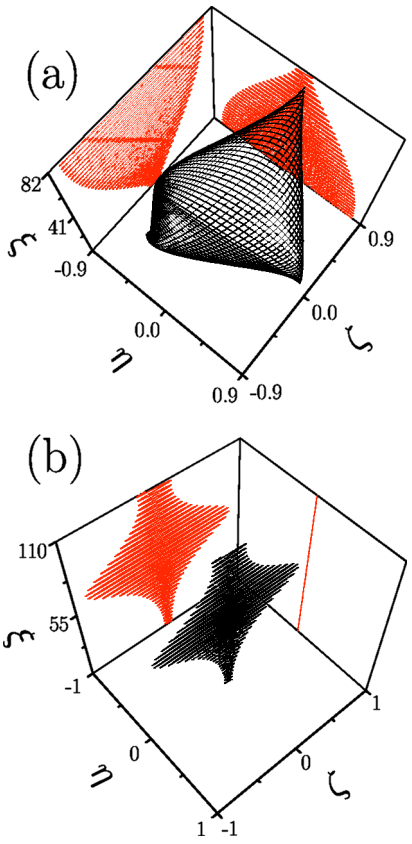

FIG. 2. (Color online). (a) Transformation of soliton center oscillations along the η axis into oscillations along the ζ axis in the harmonic lattice without longitudinal refractive index modulation at $\Omega_\eta=\Omega_\zeta=1$ and $p=5.8$. Input conditions are $\eta_0=0.8$, $\zeta_0=0.08$, $\alpha_\eta=\alpha_\zeta=0$. (b) Resonant parametric amplification of soliton oscillations along the ζ axis in longitudinally modulated Bessel lattice at $b_{\rm lin}=1.172$, $p=5$, $\mu=0.1$. Input conditions are $\eta_0=0$, $\zeta_0=0.05$, $\alpha_\eta=\alpha_\zeta=0$. In (a) and (b) soliton beams correspond to $b=7$ and $S=0.1$. All quantities are plotted in arbitrary dimensionless units.

Another opportunity to avoid the coupling between η- and ζ oscillations is related with "selective" amplification of oscillations in only one of the transverse directions. This becomes possible when the frequencies of free oscillations for orthogonal axes are different (as in a harmonic lattice

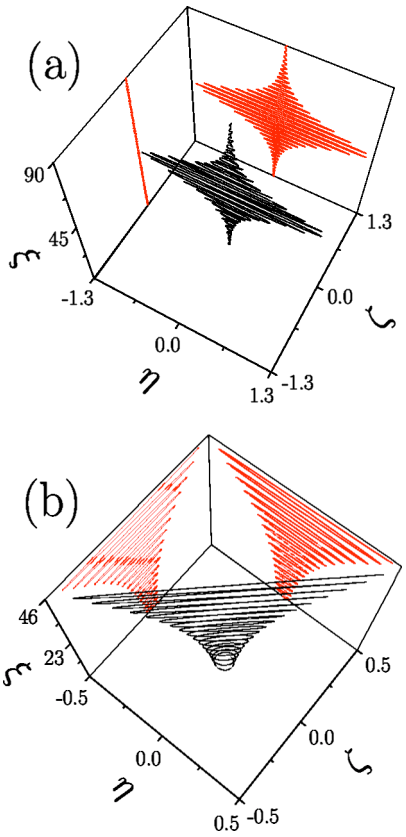

FIG. 3. (Color online). (a) Selective resonant parametric amplification of soliton oscillations along the η axis in longitudinally modulated harmonic lattice at $\Omega_\eta=1$, $\Omega_\zeta=1.5$, $p=5.8$, $\mu=0.2$. Input conditions are $\eta_0=\zeta_0=0.01$, $\alpha_\eta=\alpha_\zeta=0$. (b) Complex soliton center trajectory in longitudinally modulated Bessel lattice at $b_{\mathrm{lin}}=1.172$, $p=5$, $\mu=0.1$. Input conditions are $\eta_0=0$, $\zeta_0=0.05$, $\alpha_\eta=0.1$, $\alpha_\zeta=0$. In (a) and (b) soliton beams correspond to $b=7$ and $S=0.1$. All quantities are plotted in arbitrary dimensionless units.

with $\Omega_\eta \neq \Omega_\zeta$) and the parametric resonance condition is fulfilled along only one axis. Figure 3(a) illustrates the process of the selective parametric amplification.

The most complicated situation occurs when the process of parametric amplification is accompanied by coupling between large-amplitude oscillations along the η- and ζ axes. To realize such a regime we shifted an input soliton along the ζ axis and simultaneously tilted it along the η axis. In the absence of longitudinal modulation a soliton follows a closed elliptical (or circular in a particular case) trajectory, thus performing steady spiraling. Parametric amplification results in growth of the radius of the spiral trajectory on the initial stage of propagation. Finally, the spiral trajectory transforms into a zigzag one, which means that oscillations along the η- and ζ axes, which were initially phase shifted by $\pi/2$, become phase matched [Fig. 3(b)]. After this stage of propagation the system escapes from the parametric resonance condition and the trajectory transforms into the elliptical one.

The parametric amplification of two-dimensional soliton oscillations can be effectively used for the detection of the very small displacement and/or tilt of the input beam. For

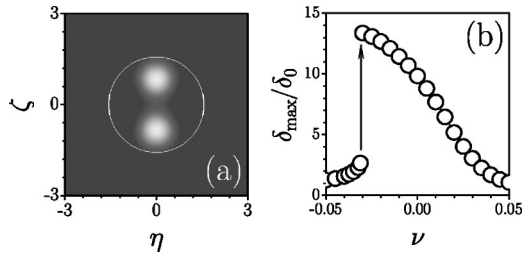

FIG. 4. (a) Snapshot images showing maximal soliton displacements in positive and negative directions of the ζ axis in longitudinally modulated Bessel lattice. Input conditions are $\eta_0=0$, $\zeta_0=0.05$, $\alpha_\eta=\alpha_\zeta=0$. (b) Maximal soliton displacement in longitudinally modulated Bessel lattice versus detuning. Input conditions are $\eta_0=0$, $\zeta_0=0.05$, $\alpha_\eta=0.1$, $\alpha_\zeta=0$. In (a) and (b) $b_{\mathrm{lin}}=1.172$, $p=5$, $\mu=0.1$, and soliton beams correspond to $b=7$ and $S=0.1$. All quantities are plotted in arbitrary dimensionless units.

instance, in the longitudinally modulated Bessel lattice the initial displacement less than 1% of the beamwidth might be amplified parametrically up to the beamwidth, as illustrated in Fig. 4(a) (the white circle shows the first zero of the Bessel lattice). Moreover, the parametric amplification can be used for fine-tuning of the output tilt angle, while selective amplification can be used to enhance soliton oscillations in the desired direction.

The key result of this work is summarized in Fig. 4(b), showing the resonance curve for transverse oscillations of a two-dimensional soliton in the longitudinally modulated Bessel lattice, i.e., dependence of the ratio between maximal $\delta_{\max}$ and input δ_0 values of transverse soliton displacement $\delta=(\langle\eta\rangle^2+\langle\zeta\rangle^2)^{1/2}$ on relative frequency detuning $\nu=(2\Omega_0-\Omega_\xi)/2\Omega_0$. This dependence has the form of a classical asymmetric parametric resonance curve for an oscillator with "soft" sine-type nonlinearity. The maximum value of parametric amplification is reached at a small negative value of frequency detuning. It should also be mentioned that the resonance curve is relatively narrow, which allows highly selective amplification. We also want to stress that, for a fixed frequency of longitudinal modulation Ω_ξ, the parametric resonance conditions can be achieved by tuning the lattice depth p, since frequency of free oscillations Ω_0 depends on the lattice depth, as follows from Eqs. (6) and (7). Notice that oscillations of two-dimensional soliton are accompanied by radiation, but its rate is substantially reduced with growth of nonlinearity saturation and soliton energy flow.

In conclusion, we showed that in harmonic and Bessel lattices imprinted in Kerr-type saturable medium it is possible to achieve considerable parametric-type amplification of soliton oscillations in the guiding lattice channel. This effect may find applications for controllable soliton steering, for detection of submicron beam displacement and extremely small misalignments.

This work has been partially supported by the Government of Spain through Grant No. BFM2002-2861 and by the Ramon-y-Cajal program.

[1] N. K. Efremidis, S. Sears, D. N. Christodoulides, J. W. Fleischer, and M. Segev, Phys. Rev. E **66**, 046602 (2002).
[2] J. W. Fleischer, T. Carmon, M. Segev, N. K. Efremidis, and D. N. Christodoulides, Phys. Rev. Lett. **90**, 023902 (2003).
[3] J. W. Fleischer, M. Segev, N. K. Efremidis, and D. N. Christodoulides, Nature (London) **422**, 147 (2003).
[4] D. Neshev, E. Ostrovskaya, Y. Kivshar, and W. Krolikowski, Opt. Lett. **28**, 710 (2003).
[5] D. N. Christodoulides, F. Lederer, and Y. Silberberg, Nature (London) **424**, 817 (2003).
[6] Y. V. Kartashov, A. S. Zelenina, L. Torner, and V. A. Vysloukh, Opt. Lett. **29**, 766 (2004).
[7] N. K. Efremidis, J. Hudock, D. N. Christodoulides, J. W. Fleischer, O. Cohen, and M. Segev, Phys. Rev. Lett. **91**, 213906 (2003).
[8] D. Neshev, A. A. Sukhorukov, Y. S. Kivshar, and W. Krolikowski, Opt. Lett. **29**, 259 (2004).
[9] J. Yang and Z. Musslimani, Opt. Lett. **28**, 2094 (2003).
[10] Z. Musslimani and J. Yang, J. Opt. Soc. Am. B **21**, 973 (2004).
[11] Y. V. Kartashov, V. A. Vysloukh, and L. Torner, Opt. Express **12**, 2831 (2004).
[12] J. Yang, I. Makasyuk, A. Bezryadina, and Z. Chen, Opt. Lett. **29**, 1662 (2004).
[13] Y. V. Kartashov, A. A. Egorov, L. Torner, and D. N. Christodoulides, Opt. Lett. **29**, 1918 (2004).
[14] Y. V. Kartashov, V. A. Vysloukh, and L. Torner, Phys. Rev. Lett. **93**, 093904 (2004); J. Opt. B: Quantum Semiclassical Opt. **6**, 444 (2004); Y. V. Kartashov, A. A. Egorov, V. A. Vysloukh, and L. Torner, Phys. Rev. E **70**, 065602(R) (2004); Y. V. Kartashov, V. A. Vysloukh, and L. Torner, Phys. Rev. Lett. **94**, 043902 (2005).
[15] Y. V. Kartashov, L. Torner, and V. A. Vysloukh, Opt. Lett. **29**, 1102 (2004).
[16] Y. V. Kartashov and V. A. Vysloukh, Phys. Rev. E **70**, 026606 (2004).